Electronic structure of hyper-kagome $Na_4Ir_3O_8$

M. R. Norman and T. Micklitz
Materials Science Division, Argonne National Laboratory, Argonne, Illinois 60439, USA
(Received 6 November 2009; revised manuscript received 11 January 2010; published 28 January 2010)

We investigate the electronic structure of the frustrated magnet $Na_4Ir_3O_8$ using density-functional theory. Due to strong spin-orbit coupling, the hyper-kagome lattice is characterized by a half-filled complex of *d* states, making it a cubic iridium analog of the high-temperature superconducting cuprates. The implications of our results for this unique material are discussed.

DOI: 10.1103/PhysRevB.81.024428 PACS number(s): 75.30.Et, 71.70.Ej, 75.10.Lp, 75.50.Ee

I. INTRODUCTION

Recently, several materials have been identified[1] as possible candidates for a long sought state of matter—the quantum spin liquid.[2] One of these candidates, $Na_4Ir_3O_8$, is characterized by a three-dimensional cubic space group, where the iridium sites form a hyper-kagome lattice of corner-sharing triangles. This remarkable material is an insulator with a large Curie-Weiss temperature (650 K) and a large effective moment ($1.96\mu_B$), yet does not exhibit any sign of magnetic order down to the lowest measured temperature.[3]

There have been a number of theoretical studies of this iridate[4] which attempt to address the nature of the spin-liquid ground state. These studies invariably assume that the material is described by an isotropic Heisenberg model since anisotropy acts to stabilize magnetic order. Isotropy would be a surprise given the strong spin-orbit coupling for the iridium ions. But in an exhaustive study, Chen and Balents[5] formulated under what conditions such an effective model might be realized. To address various issues raised in that paper, we calculated the electronic structure of this material within the local-density approximation (LDA), then performed a tight-binding fit in order to estimate the various exchange integrals which enter the spin Hamiltonian for this frustrated magnet. We find that the spin Hamiltonian should be strongly anisotropic but offer two possible scenarios where isotropy might be restored.

II. CALCULATIONAL DETAILS

Although $Na_4Ir_3O_8$ has a cubic space group, the unit cell is quite complicated, comprising four formula units (60 atoms).[3] Moreover, the lattice breaks inversion symmetry. The space group, $P4_132$, is also found in the noncentrosymmetric superconductors Li_2Pd_3B and Li_2Pt_3B.[6] The material is formed from distorted IrO_6 octahedra, each comprised of two different oxygen sites—four of type 2 (O2) and two of type 1 (O1). The latter should not be thought of as "apical" oxygens in the cuprate sense since they are not related by inversion through the iridium site. Rather, each octahedron is described by a C_2 axis along a (110) direction.[5] There are 12 of these axes, one associated with each of the 12 iridium ions in the unit cell. Each oxygen ion is also at the center of a distorted octahedron, with O1 octahedra of the form OIr_3Na_3, and O2 octahedra of the form OIr_2Na_4. Each oxygen ion is also surrounded by a very distorted array of 12 other oxygen ions along approximate (110) directions. Finally, each iridium ion is surrounded by four other iridium ions, also along approximate (110) directions. These form the corner-sharing triangles that characterize the hyper-kagome lattice. A list of the first few coordination shells around an iridium ion is given in Table I.

When considering an electronic-structure calculation for this material, the first issue is that there are three different types of sodium ions, two of which are partially occupied with a stochiometry of 75%.[3] Therefore, to form a simple unit cell, some approximation has to be made for these other two sodium sites. We choose to fully occupy the 12*d* sites (sodium type 3) and replace the 4*a* sites (sodium type 2) by empty spheres. The resulting lattice has 64 sites in the unit cell—12 Ir, 8 O1, 24 O2, 4 Na1, 4 empty (i.e., Na2), and 12 Na3.

The calculations in this paper were performed using the LDA within a linear muffin-tin-orbital scheme.[7] Overlap (combined) corrections were incorporated but the Coulomb potential at each site was treated in a spherical approximation. The exchange-correlation potential used was that of Hedin and Lundqvist.[8] Noting that the cubic lattice constant is 8.985 Å, a muffin-tin radius of 1.238 Å was used on the iridium sites, and 1.425 Å was used on all other sites. These

TABLE I. Coordination shells around an iridium ion in the $Na_4Ir_3O_8$ structure out to a distance of 0.49*a*. Listed is the type of ion, their number, (approximate) direction, and distance (in units of the lattice constant, *a*).

Type	Number	Direction	Distance
O2	2	100	0.2273
O2	2	100	0.2280
O1	2	100	0.2333
Ir	4	110	0.3464
Na3	2	110	0.3501
Na3	2	110	0.3587
Na1	2	110	0.3612
Na3	1	110	0.3627
Na2	1	110	0.3683
O2	2	111	0.4065
O2	2	111	0.4225
O1	2	111	0.4375
O2	2	111	0.4838

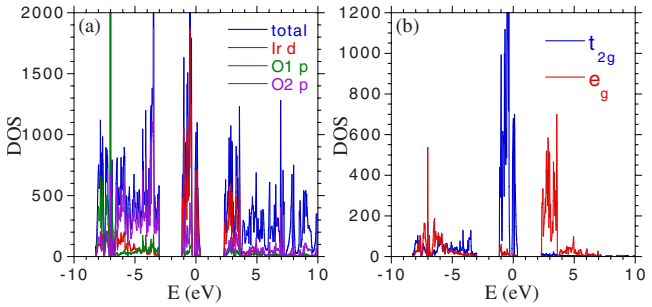

FIG. 1. (Color online) DOS in states/Ryd for the scalar relativistic calculation of $Na_4Ir_3O_8$. The Fermi energy, E_F, is at zero.

radii were chosen based on the various near-neighbor separations. *s* and *p* basis functions were used on all sites (including the empty ones) except for the iridium sites, where *d* basis functions were also included. For the scalar relativistic calculation (all relativistic effects but spin orbit), this resulted in a secular matrix of dimension 316, which was double this (632) for the full relativistic (Dirac equation) calculation. The calculations were converged using 56 *k* points in the irreducible wedge of the Brillouin zone. We should note that the Brillouin zone for this material is simple cubic. Though inversion symmetry is broken, one can restrict the irreducible wedge to 1/48th of the zone. The eigenvalues at a general *k* point are doubly (Kramers) degenerate unless spin orbit is incorporated, where this degeneracy is broken. After convergence, 165 *k* points were generated in the irreducible wedge. The eigenvalues were then fit using a Fourier spline series[9] with 560 lattice periodic functions. A linear tetrahedron method[10] was used to evaluate the density of states (DOS), with the zone broken down into 48×8^5 tetrahedra.

III. RESULTS

We first present results from the scalar relativistic calculation, with the density of states shown in Fig. 1. The O1 states form a narrow complex of bands ranging from −8.2 to −6.7 eV, followed by the wider O2 complex ranging from

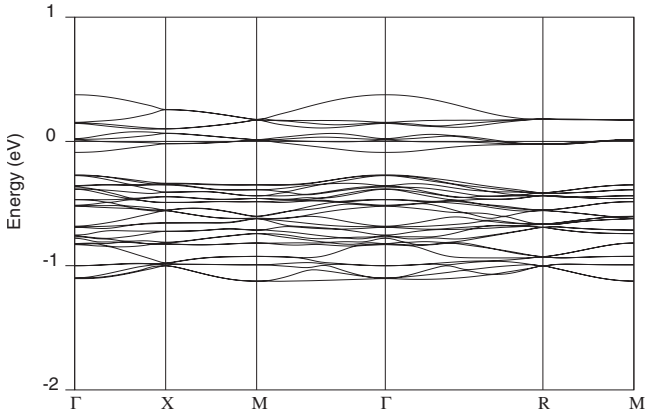

FIG. 2. Energy bands of the t_{2g} complex for the scalar relativistic calculation of $Na_4Ir_3O_8$. $\Gamma=(0,0,0)$, $X=(1,0,0)$, $M=(1,1,0)$, and $R=(1,1,1)$ in units of π/a. The horizontal line marks E_F.

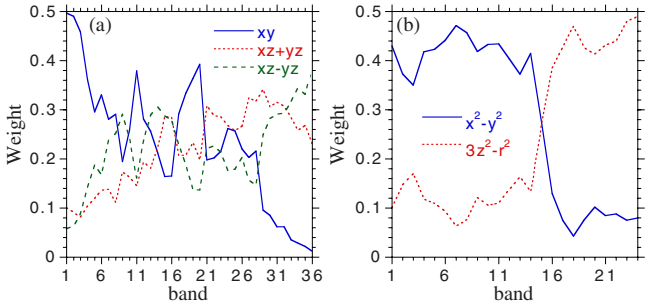

FIG. 3. (Color online) Decomposition of the (a) t_{2g} states and (b) e_g states, averaged over each band, into their individual components relative to the C_2 axis of the distorted IrO_6 octahedra (scalar relativistic calculation).

−6.7 to −3 eV (there is only a narrow gap between these two complexes). There is a gap of 1.9 eV to the t_{2g} complex of iridium *d* bands ranging from −1.1 to 0.4 eV. This is followed by a crystal field gap of 1.9 eV to an e_g complex ranging from 2.3 to 3.6 eV. For energies above this, the states are primarily from the sodium sites. The main complex of interest is the t_{2g} one (Fig. 2). It is split into an array of 28 bands (each Kramers degenerate) separated by a gap of 0.2 eV to an upper array of eight bands. This basic splitting of 28 and 8 arises from the t_{pd} hopping integral, as identified from tight-binding fits, and is related to the fourfold degeneracy of the eigenvalues at the *R* point of the zone. There is a crystal field splitting of the t_{2g} states which was identified by projecting onto the three crystal-field components due to the C_2 axis, with the *xy* states (for a 110 axis) lying lowest in energy but it is rather ill defined (Fig. 3) and is small relative to the overall t_{2g} bandwidth. The t_{2g} complex is composed of 70% Ir 5*d* character, 20% O2 2*p* character, and 4% O1 2*p* character. The centroid of the e_g complex relative to the t_{2g} one is 3.5 eV, with the t_{2g}-e_g admixture (due to the low iridium-site symmetry) quite small. The density of states at the Fermi energy (per Ir per spin) is 3.35 states/eV. The Fermi surface (not shown) is composed of small pockets, two about the *R* point (electronlike), two about the *M* point (holelike), and one around the Γ point (holelike).

Spin-orbit coupling has a profound impact on these results, as can be seen in the remaining figures. The t_{2g} states now split (Figs. 4 and 5) into a lower complex of 48 bands and an upper complex of 24 bands (the number of bands are now doubled because of the coupling of inversion breaking

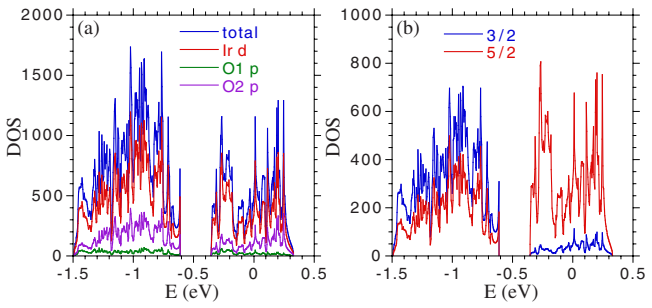

FIG. 4. (Color online) DOS in states/Ryd for the full relativistic calculation of $Na_4Ir_3O_8$.

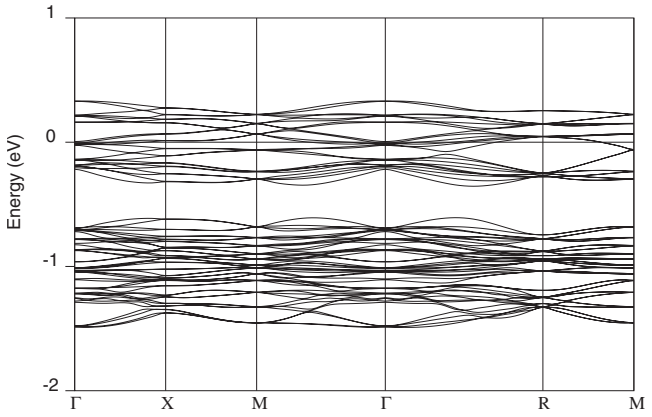

FIG. 5. Energy bands of the t_{2g} complex for the full relativistic calculation of $Na_4Ir_3O_8$. The horizontal line marks E_F.

with spin orbit), with the e_g complex composed of another 48 bands. The upper t_{2g} complex is half filled, with the Ir d states mostly of $j=5/2$ character, with weak admixture of $j=3/2$ character (Fig. 4). As explained by Chen and Balents,[5] and found as well for the electronic structure of Sr_2IrO_4,[11] this behavior is due to crystal-field admixture of the $j=5/2$ and $j=3/2$ states, which acts to form a mixed lower (t_{2g}) quartet of states (i.e., four per iridium site), a mixed (e_g) upper quartet, with an unmixed (t_{2g},$j=5/2$) doublet in between that is half filled. This doublet is predicted to have 83% $j=5/2$, $m_j=\pm 3/2$ and 17% $j=5/2$, $m_j=\pm 5/2$ character, which is in good agreement with the results we find for the lowest eight bands of this complex (Fig. 6). The upper 16 bands have a slightly reduced $m_j=\pm 3/2$ weight due to weak admixture with $m_j=\pm 1/2$ states as well as $j=3/2$ states, which is a consequence of the low iridium-site symmetry. Again, the density of states at the Fermi energy is not large—per Ir per spin it is 1.51 states/eV. The Fermi surface is composed of three electronlike sheets around Γ, and two holelike sheets around the R point (Fig. 7). The bands are doubly degenerate on the zone face due to the nonsymmorphic nature of the space group.

We now wish to connect these results to the insulating behavior of the actual material. In the case of Sr_2IrO_4, inclusion of the Coulomb repulsion is not sufficient to open an energy gap unless spin orbit is included. In essence, spin orbit produces a half-filled doublet which can then "Mott-Hubbardize" and form an insulator, similar to what occurs in the cuprates.[12] Only a small U is needed to cause this.[11] Similar considerations should apply to $Na_4Ir_3O_8$. From the centroids of the two quartets and the doublet, we have inferred the parameters Δ_{CF} (splitting of t_{2g} and e_g) and λ (coefficient of $\mathbf{l}\cdot\mathbf{s}$ for the spin-orbit coupling) of 3.43 and 0.58 eV, respectively.

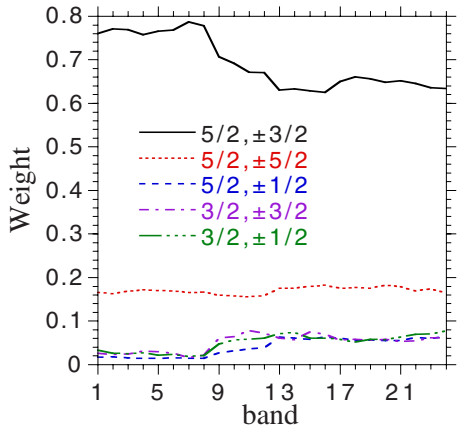

FIG. 6. (Color online) Decomposition of the states of the upper t_{2g} "doublet" complex, averaged over each band, into their atomic spin-orbit components, $j,\pm m_j$ (full relativistic calculation). The weights are normalized to the total d weight.

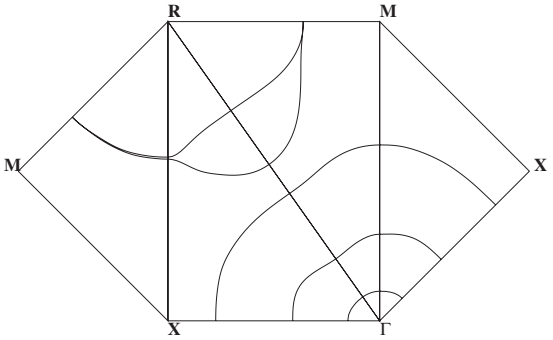

FIG. 7. Fermi surface for the full relativistic calculation of $Na_4Ir_3O_8$ in the symmetry planes of the zone.

IV. TIGHT-BINDING ANALYSIS

To investigate these issues further, we performed tight-binding fits to the electronic structure, restricting to Ir 5d and O 2p orbitals. This involved generating Slater-Koster parameters[13] and then performing a least-squares fit to the band eigenvalues using Powell's method.[14] Because of the distorted nature of the lattice, there are a large number of tight-binding parameters, even if one restricts to near neighbors. This is because there is not a unique distance for several of the atom combinations (Ir-O2, O1-O1, O1-O2, and O2-O2). To compensate for this, we assumed that the tight-binding parameters for each atom combination vary as the fourth power of the distance. This assumption works well for the O-O hoppings in IrO_2 (Ref. 15) (note from Table I that the two Ir-O2 distances are almost identical). This reduced us to four t_{pd} parameters (σ and π for Ir-O1 and Ir-O2), three t_{dd} parameters (σ, π, and δ for Ir-Ir), six t_{pp} parameters (σ and π for O1-O1, O1-O2, and O2-O2), four on-site energies (2p energies for O1 and O2, and t_{2g} and e_g energies), and the spin-orbit coupling of the Ir d (λ), for a total of 18 parameters. We have explored putting in the residual crystal field splittings due to the low Ir site symmetry (Fig. 3) but this did not lead to improved fits.

We first converged the fit for the scalar relativistic calculation, using 42 eigenvalues (top and bottom of the O1 complex, O2 complex, e_g complex, and all 36 t_{2g} bands) at the four symmetry points (Γ, X, M, and R). As input, we used IrO_2 hopping parameters[15] scaled to the sodium iridate distances, as well as on-site energies estimated from averages extracted from the l decomposed density of states. The fit (not shown) yielded a band structure in good agreement with Fig. 2. We then used these fit parameters as input to fitting

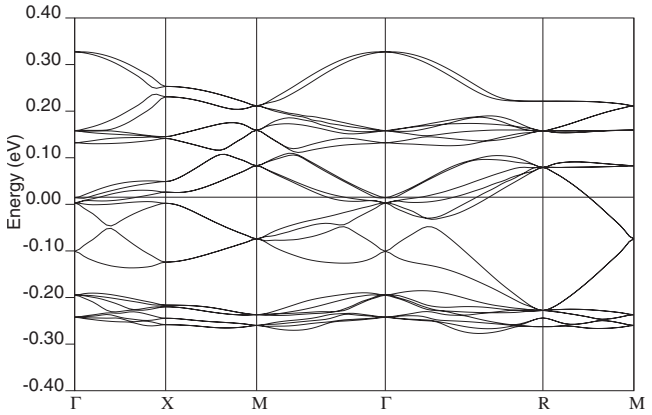

FIG. 8. Energy bands for the upper t_{2g} doublet complex from the tight-binding fit to the full relativistic calculation of $Na_4Ir_3O_8$. The horizontal line marks E_F.

the full relativistic calculation, with the same set of eigenvalues (now numbering 78) at each of the four k points. The fit gives a good description of the bands and Fermi surface, as can be seen in Figs. 8 and 9. These fit values are listed in Table II. One can see that the t_{pd} and t_{dd} parameters have comparable magnitude, and that the O1 and O2 integrals are quite different. Note that the difference of the t_{2g}-e_g energies is only 2.60 eV. The difference from the centroid splitting of 3.43 eV quoted earlier is due to the contribution of the hoppings to the splitting.

V. EXCHANGE INTEGRALS

As we are in the strong spin-orbit coupling limit in the sense of Chen and Balents,[5] we can use the expressions in their paper to estimate the various exchange integrals (Table III). We caution that these values are very sensitive to the tight-binding parameters, as well as the values of the Coulomb U. The exchange Hamiltonian is of the form[5]

$$H_{ex} = (J_d + J_s)\mathbf{S}_n \cdot \mathbf{S}_m + \mathbf{D}^{nm} \cdot (\mathbf{S}_n \times \mathbf{S}_m) + \mathbf{S}_n \cdot \mathbf{\Gamma}^{nm} \cdot \mathbf{S}_m, \tag{1}$$

where J_d is the direct exchange between iridium ions, J_s the isotropic component of the superexchange mediated by the oxygen ions, D the Dzyaloshinski-Moriya interaction, and Γ the anisotropic part of the superexchange.

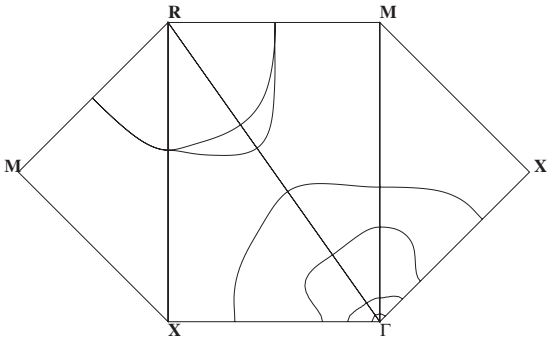

FIG. 9. Fermi surface from the tight-binding fit to the full relativistic calculation of $Na_4Ir_3O_8$.

TABLE II. Tight-binding hopping parameters in eV. The on-site energies are $\epsilon_{O1}=-5.1913$, $\epsilon_{O2}=-4.0954$, $\epsilon_{t_{2g}}=-1.7983$, and $\epsilon_{e_g}=0.7987$, with the spin-orbit coupling $\lambda=0.6386$.

	σ	π	δ
Ir-O1	−2.5579	0.3186	
Ir-O2	−2.1070	1.1817	
Ir-Ir	−0.6372	0.0719	0.1545
O1-O1	0.6156	0.0354	
O2-O2	0.5463	−0.2121	
O1-O2	−1.1327	0.0663	

Remarkably, for the direct Ir-Ir exchange, we find that even for the distorted lattice, the interaction is isotropic, and is given by the simple formula $J_d=2t^2/U$, where $t=\frac{1}{4}t_{dd}^{\sigma}+\frac{1}{3}t_{dd}^{\pi}+\frac{5}{12}t_{dd}^{\delta}$. The value we find is sizable, about 20 meV, which is not so different from the experimental estimate of 28 meV.[3] It would be larger, except for the anomalously large value of t_{dd}^{δ}. In that context, we remark that these hoppings are effective values and compensate for the fact that we only include 18 tight-binding parameters in our fits. For instance, in the more complete analysis Mattheiss did for the simpler IrO_2, t_{dd}^{δ} is only about 6% of t_{dd}^{σ}.[15] We have done a tight-binding fit including the residual crystal-field splittings (Fig. 3) which did have a much reduced value for t_{dd}^{δ} (with a larger value for J_d of 37 meV) but the Fermi surface was degraded in this fit.

We now turn to the superexchange, which is responsible for all values of the exchange Hamiltonian except for J_d. The values (Table III) are large and highly anisotropic (we should caution, though, that these values will be further affected by the t_{pp} hoppings[16]). This is unlike what would occur if the local site symmetry of the Ir ions was purely cubic.[17] The large values are not only due to the distortion of the octahedra but also because the superexchange between two given Ir ions is mediated by an O1 and an O2 ion, each of which is in a different environment (Fig. 10). For instance, the nonzero values of J_s, D, and the off-diagonal components of Γ are due to the distortion, with the magnitude strongly influenced by the difference between the O1 and O2 ions. On the other

TABLE III. Exchange integrals in meV. The spin Hamiltonian is given in Eq. (1). Quoted are values where Ir site m is along an $(0,1,-1)$ direction relative to Ir site n. D are the Dzyaloshinski-Moriya and Γ the anisotropic superexchange terms (in the second row for Γ, the jk refer to the parenthesis, xy, etc.). In addition, the direct exchange is $J_d=20.1$ and the isotropic superexchange term is $J_s=12.9$. The last row, J_{ii}, is the total exchange for the diagonal components ($J_d+J_s+\Gamma_{ii}$). The assumed value of U is 0.5 eV (Ref. 11) (with U_p set to zero).

$i(jk)$	$x(xy)$	$y(xz)$	$z(yz)$
D_i	47.3	1.3	−4.7
Γ_{ii}	36.1	−36.8	−36.2
Γ_{jk}	2.1	−8.3	−0.2
J_{ii}	69.2	−3.7	−3.1

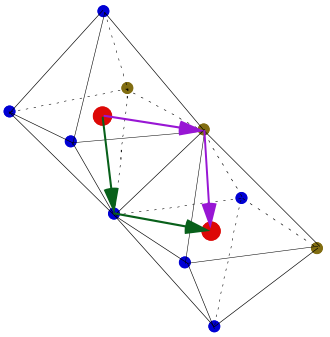

FIG. 10. (Color online) Superexchange pathway between two Ir ions as marked by the arrows. The Ir ions are the large (red) spheres and the oxygen ions the small ones. The lower left (green) pathway is via an O2 (blue) ion and the upper right (purple) pathway via an O1 (brown) ion.

hand, the reversed sign of the diagonal components of Γ relative to the cubic model of Chen and Balents[5] is due to the difference between O1 and O2, with the magnitude little affected by the distortion.

There are only two ways we know to reduce these large values of the superexchange. First, in the limit of large U_p (Coulomb repulsion on the oxygen sites), they would vanish. Second, because the sodium sites about the oxygens are only partially occupied in the real material, it is possible that the resulting randomness would dephase the various superexchange pathways. Unless one of these mechanisms is effective, the total exchange is predicted to be anisotropic. This would cast doubts on theories for $Na_4Ir_3O_8$ based on an isotropic Heisenberg model. Regardless, we believe that the tight-binding parameters we provide here will be useful for future modeling of this fascinating material. In particular, given the resemblance of its electronic structure to that of cuprates, one might wonder whether a doped version of this material would be a high-temperature superconductor.

ACKNOWLEDGMENTS

Work at Argonne National Laboratory was supported by the U.S. DOE, Office of Science, under Contract No. DE-AC02-06CH11357.

[1] P. A. Lee, Science **321**, 1306 (2008).
[2] P. W. Anderson, Mater. Res. Bull. **8**, 153 (1973).
[3] Y. Okamoto, M. Nohara, H. Aruga-Katori, and H. Takagi, Phys. Rev. Lett. **99**, 137207 (2007).
[4] J. M. Hopkinson, S. V. Isakov, H.-Y. Kee, and Y. B. Kim, Phys. Rev. Lett. **99**, 037201 (2007); M. J. Lawler, H.-Y. Kee, Y. B. Kim, and A. Vishwanath, *ibid.* **100**, 227201 (2008); M. J. Lawler, A. Paramekanti, Y. B. Kim, and L. Balents, *ibid.* **101**, 197202 (2008); Y. Zhou, P. A. Lee, T.-K. Ng, and F.-C. Zhang, *ibid.* **101**, 197201 (2008).
[5] G. Chen and L. Balents, Phys. Rev. B **78**, 094403 (2008).
[6] K.-W. Lee and W. E. Pickett, Phys. Rev. B **72**, 174505 (2005).
[7] O. K. Andersen, Phys. Rev. B **12**, 3060 (1975).
[8] L. Hedin and B. I. Lundqvist, J. Phys. C **4**, 2064 (1971).
[9] D. D. Koelling and J. H. Wood, J. Comput. Phys. **67**, 253 (1986).
[10] G. Lehmann and M. Taut, Phys. Status Solidi **54**, 469 (1972).
[11] B. J. Kim, H. Jin, S. J. Moon, J.-Y. Kim, B.-G. Park, C. S. Leem, J. Yu, T. W. Noh, C. Kim, S.-J. Oh, J.-H. Park, V. Durairaj, G. Cao, and E. Rotenberg, Phys. Rev. Lett. **101**, 076402 (2008); H. Jin, H. Jeong, T. Ozaki, and J. Yu, Phys. Rev. B **80**, 075112 (2009).
[12] P. W. Anderson, Science **235**, 1196 (1987).
[13] J. C. Slater and G. F. Koster, Phys. Rev. **94**, 1498 (1954).
[14] W. H. Press, B. P. Flannery, S. A. Teukolsky, and W. T. Vetterling, *Numerical Recipes* (Cambridge University Press, Cambridge, 1989). The function being minimized is a sum of the squares of the differences of the tight binding and band eigenvalues.
[15] L. F. Mattheiss, Phys. Rev. B **13**, 2433 (1976).
[16] A. Shitade, H. Katsura, J. Kunes, X.-L. Qi, S.-C. Zhang, and N. Nagaosa, Phys. Rev. Lett. **102**, 256403 (2009).
[17] D. Podolsky and Y. B. Kim, arXiv:0909.4546 (unpublished).